81. MAGNETOHYDRODYNAMICAL MODELS OF HELICAL MAGNETIC FIELDS IN SPIRAL ARMS

M. FUJIMOTO
Nagoya University, Nagoya, Japan
and
M. MIYAMOTO
Tokyo Astronomical Observatory, Tokyo, Japan

Abstract. A circular arm with elliptical cross-section is used as a model of the spiral arm. It is demonstrated magnetohydrodynamically that interstellar gas may flow in a helical path along the axis of the arm and interstellar helical magnetic lines of force can spiral around it. It is pointed out that though the rolling motions of gas do not always indicate the existence of the helical magnetic field, the latter cannot be in a stationary state without the former. Some observational supports to the present model are given.

1. Motions of Gas in a Spiral Arm

A circular arm is assumed as a model of the spiral arm, whose density ϱ_s is uniform and whose cross-section is elliptical with semi-major axis, a, in the galactic plane and semi-minor axis, b, perpendicular to it. As shown in Figure 1, a local Cartesian coordinates system (x,y,z) is introduced with the origin at the arm axis which is situated at galactocentric distance r_0. This local coordinate system rotates in the direction of the y-axis with the angular velocity Ω of galactic rotation at $r=r_0$. Since $r_0 \gg a$, b, in general, we can restrict our discussions only to a small portion of the galaxy near the arm axis. In deriving equations of motion of gas, we expand the pressure and gravitational forces in Taylor series around the arm axis, and take the first two terms. The first term balances the centrifugal force due to the rotation of the local coordinate

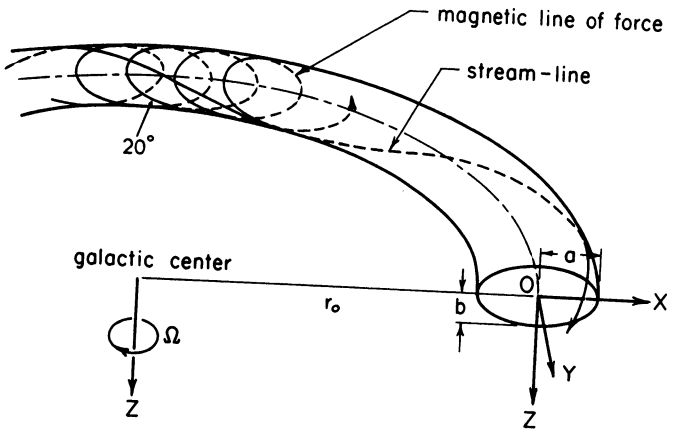

Fig. 1. Helical magnetic fields and rolling motions of the gas.

Becker and Contopoulos (eds.), The Spiral Structure of Our Galaxy, 444–447.

system, and the second term is linear in x and z. Then the y- and time-independent equations of motion are written as follows,

$$U_x \frac{\partial U_x}{\partial x} + U_z \frac{\partial U_x}{\partial z} = 2\Omega U_y - C \cdot x + F_1 , \tag{1}$$

$$U_x \frac{\partial U_y}{\partial x} + U_z \frac{\partial U_y}{\partial z} = -2\Omega U_x + F_2 , \tag{2}$$

and

$$U_x \frac{\partial U_z}{\partial x} + U_z \frac{\partial U_z}{\partial z} = -D \cdot z + F_3 , \tag{3}$$

where C and D are constants evaluated at $r = r_0$ and F_1, F_2, and F_3 are accelerations due to the Lorentz force. It has been shown by Fujimoto and Miyamoto (1969) that the following motion and helical field satisfy Equations (1)–(3),

$$\mathbf{U} = (Lz, Mx, Nx) \tag{4}$$

$$\mathbf{B} = (B_* Lz, B_0 + B_* Mx, B_* Nx), \quad \text{for} \quad (x^2/a^2) + (z^2/b^2) \leqslant 1 , \tag{5}$$

and

$$\mathbf{B} = 0, \quad \text{for} \quad (x^2/a^2) + (z^2/b^2) > 1 , \tag{6}$$

where L, M, N and B_* are constants still to be determined by Equations (1)–(3), and B_0 denotes a uniform field parallel to the arm. In an inertial frame, the motion $U_x = Lz$, $U_y = Mx$ and $U_z = Nx$ gives a helical motion along the arm. Note that we have $\mathrm{rot}(\mathbf{U} \times \mathbf{B}) = 0$ and $\mathbf{U} \times \mathbf{B} \neq 0$ for $\mathbf{U}$ and $\mathbf{B}$ in Equations (4)–(6). Substituting Equations (4)–(6) in Equations (1)–(3), we have, in the case of the tightly wound helical fields,

$$L = \pm \frac{a}{b} \sqrt{D} (1 - E_{\mathrm{Mg}}/E_{\mathrm{K}})^{-1/2} \tag{7}$$

$$M = -2\Omega (1 - E_{\mathrm{Mg}}/E_{\mathrm{K}})^{-1} , \tag{8}$$

and

$$N = \mp \frac{b}{a} \sqrt{D} (1 - E_{\mathrm{Mg}}/E_{\mathrm{K}})^{-1/2} , \tag{9}$$

with the constraint on the model,

$$D - C = 4\Omega^2 (1 - E_{\mathrm{Mg}}/E_{\mathrm{K}})^{-1} . \tag{10}$$

which implies that stream lines are closed in the local coordinate system. We have the following identities,

$$\frac{E_{\mathrm{Mg}}}{E_{\mathrm{K}}} = \frac{B_*^2}{4\pi \varrho_{\mathrm{s}}} = \frac{\text{Energy density of the poloidal components of the helical field}}{\text{Energy density of the poloidal components of the rolling motion of the gas}} .$$

https://doi.org/10.1017/S0074180900001017 Published online by Cambridge University Press

TABLE I

Velocities of rolling motions of gas and helical magnetic field for various values of E_{Mg}/E_K

	E_{Mg}/E_K				
	0.0	0.1	0.3	0.5	0.7
U_x	$\pm 8.0z$ km s^{-1}	$\pm 10.0z$	$\pm 15.5z$	$\pm 25.1z$	$\pm 46.6z$
U_y	$-5.0z$	$-5.5x$	$-7.1x$	$-10.0x$	$-16.7x$
U_z	$\mp 0.9x$	$\mp 1.1x$	$\mp 1.7x$	$\mp 2.8x$	$\mp 5.2x$
B_x	0	$\pm 2.1\times10^{-6}z$ G	$\pm 5.6\times10^{-6}z$	$\pm 1.2\times10^{-5}z$	$\pm 2.6\times10^{-5}z$
B_y	0	$-1.1\times10^{-6}x$	$-2.6\times10^{-6}x$	$-4.6\times10^{-6}x$	$-9.1\times10^{-6}x$
B_z	0	$\mp 2.3\times10^{-7}x$	$\mp 6.2\times10^{-7}x$	$\mp 1.3\times10^{-6}x$	$\mp 2.8\times10^{-6}x$
$\sqrt{\langle v_2\rangle}$	9.5 km s^{-1}	9.5	9.1	8.1	5.2

(1) x and z are measured in 100 pc; (2) $\sqrt{\langle v^2\rangle}$ is the root mean square molecular (or random) velocity of the gas at the arm axis; (3) the constant B_* is taken as positive. When it is negative, the signs in B_x, B_y and B_z are to be reversed.

Table I lists numerical solutions for the characteristics of the models of the arm at $r_0=10$ kpc in our Galaxy, in which we have assumed $\varrho_s=2$ hydrogen atoms cm^{-3} and $b/a=1/3$ with $a=250$ pc. The uniform component B_0 can be estimated from the observed pitch angle of the helical field. They are about $B_0=3\times10^{-7}\sim2\times10^{-6}$ G, corresponding to $E_{Mg}/E_K=0.1\sim0.7$ in Table I. We find from Table I that the velocities of the rolling motion and the magnitudes of the helical field amount to $10\sim20$ km s^{-1} and $10^{-6}\sim10^{-5}$ G, respectively, near the arm surface.

2. Conclusions and Comparisons with Observations

Magnetohydrodynamical treatments have been made on interstellar helical magnetic fields in a spiral arm. It is concluded that interstellar gas can flow in a helical path around the arm axis and that a stationary helical magnetic field can be maintained with such rolling motions. The helical magnetic field as well as the velocity field in our stationary model are demonstrated schematically in Figure 1. Equations (7)–(9) show that rolling motions in the gas do not always indicate the existence of a helical field.

It is possible to compare the present models with observations of the peculiar motions of the gas and with the local magnetic fields in spiral arms in our galaxy. The neutral hydrogen gas in the 4-kpc arm exhibits a rolling motion, as first found by Oort. This same type of motion has been found in the Perseus arm by Westerhout (1970) and Kerr (1970). The velocity difference in the line-of-sight component amounts to $|\delta v_r|\simeq20$ km s^{-1} above and below the galactic plane in the region $l^{II}=110°\sim130°$. Velden (1970) has observed radial velocities of neutral hydrogen gas in intermediate latitudes ($|b^{II}|=10°\sim30°$) toward the direction of the galactic anti-center. The radial velocities take the values ∓4.5 km s^{-1} for $b^{II}=10°\sim30°$ and

https://doi.org/10.1017/S0074180900001017 Published online by Cambridge University Press

$b^{II} = -10° \sim -30°$, respectively; this implies the existence of rolling motions, at least, in the solar neighbourhood. The sense of this motion is that of a right-handed helix in both the Orion and the Perseus arms. The velocities of these rolling motions are compatible with those derived in the present models (see Table I).

Mathewson (1968) has combined his polarization data on 1400 stars with those measured in the northern hemisphere, to deduce a magnetic field model for the solar vicinity. His model construction was carried out by trial and error with different configurations until a good approximation was obtained to the observed *E*-vector distribution for polarized starlight. The best model, in which magnetic field lines are tightly wound around the spiral arm, can explain not only the distribution of the *E*-vectors, but also sign-reversals of rotation measures for polarized extragalactic radio sources outside the galactic plane and polarization planes for the non-thermal galactic radio continuum. Since Mathewson has already made extensive comparisons between his helical field models and the observations, and has obtained good fits, we need not discuss these in more detail. We shall, however, point out some differences between these models and those discussed in the present paper.

The helical pattern in the Mathewson's models is sheared through an angle of 40° in the galactic plane, in a counter-clockwise sense when viewed from the north pole, and it is vertical to the galactic plane. In the present models, on the other hand, the helical pattern is not sheared and it is tilted with respect to the galactic plane by an angle of 20° (Figure 1). Another discrepancy between observations and the results of the present model is observed in the positions of sign-reversal for the rotation measures. Actual sign reversals are observed at $l^{II} \sim 40°$ and $\sim 220°$ (Gardner and Davies, 1966; Berge and Seielstad, 1967; Gardner *et al.*, 1967), while the theory presented here predicts directions of $l^{II} \sim 0°$ and $\sim 180°$.

Many other observational characteristics of the local magnetic field can be explained by the present model.

A more extended paper with the same title has been published in *Publ. Astron. Soc. Japan* (Fujimoto and Miyamoto, 1969).

References

Berge, G. L. and Seielstad, G. A.: 1967, *Astrophys. J.* **148**, 367.
Fujimoto, M. and Miyamoto, M.: 1969, *Publ. Astron. Soc. Japan* **21**, 194.
Gardner, F. F. and Davies, R. D.: 1966, *Australian. J. Phys.* **19**, 129.
Gardner, F. F., Whiteoak, J. B., and Morris, D.: 1967, *Nature* **214**, 371.
Kerr, F. J.: 1970, IAU Symposium No. 38, p. 95.
Mathewson, D. S.: 1968, *Astrophys. J.* **153**, 447.
Velden, L.: 1970, IAU Symposium No. 38, p. 164.
Westerhout, G.: 1970, IAU Symposium No. 38, p. 122.